3NM4 Application Demonstration

William Ward 400170514

Fall 2021

1 Problem Statement

I have chosen to focus on solving a second order linear ordinary differential equation that describes the potential energy within the depletion region of a p-n junction in the steady-state. From Maxwell's equations, the potential energy within the depletion region of a p-n junction is defined by Poisson's equation (1).

$$\frac{\partial^2 U}{\partial x^2} = \frac{\rho}{\epsilon\epsilon_0} \tag{1}$$

Where ρ is the charge density within the region. It is often the case that the charge density within the depletion portion of both the p-doped and n-doped material is approximated as the carrier concentration. Thus, the charge density is a piece-wise function of x.

$$\rho(x) = \begin{cases} eN_A, & -d_A < x < 0 \\ -eN_D, & 0 < x < d_D \end{cases} \tag{2}$$

Where N_A is the acceptor concentration, N_D is the donor concentration, e is the fundamental charge and the depletion region ranges from $-d_A$ to d_D. The physical layout of this problem is shown below in figure (8) in the appendix. Special consideration will have to be given to the interface between the P & N region as the differential equations within each region are different. The given boundary conditions are outlined below.

$$\begin{cases} U(-d_A) = 0 \\ U(d_D) \quad = U(n) \end{cases} \tag{3}$$

In addition, since the differential equation that describes the potential in each side of the depletion region is different (since $N_A \neq N_D$ necessarily), we require that the solutions be equal in value and 1st derivative at the boundary.

$$\left\{ \begin{array}{l} U_A(0) = U_D(0) \\ \frac{\partial U_A}{\partial x}\big|_0 = \frac{\partial U_D}{\partial x}\big|_0 \end{array} \right\} \tag{4}$$

Finally, the problem must satisfy the following equation by charge neutrality.

$$d_A N_A = d_D N_D \tag{5}$$

The given values in this problem are: the band gap energy $U(n)$, the carrier concentrations N_A & N_D, and the depletion region widths d_A & d_D. The problem requires that I find the potential energy at the interface between the P & N regions, when the carrier concentrations are different (i.e. one side is heavily doped). The appropriate constants are given in the appendix (17).

2 MATLAB Code

In order to solve this problem, I discretized the region, and applied finite difference approximations to the differential equations. In order to demonstrate the utility of finite difference methods, I also implemented a more difficult shooting solution. The finite difference method allowed me to solve the problem using a linear system of equations. The general node equations were then developed for both the N and P regions. The node at the interface between the regions was expressed by applying finite difference approximations within the appropriate region. It is important to note that this required a forward difference approximation for one side of the equation, and a backward difference approximation for the other side of the equation. The boundary conditions were simply applied in the constant vector b. The node equations and applied boundary conditions are written out in the appendix for brevity (see equations (6 - 14)). The shooting solution was implemented by manually updating the guess for $\frac{\partial U}{\partial x}\big|_{-d_A}$ using the secant method (see equation (16)). A new solution was obtained after each WAG update using $ode45$ (recall that $ode45$ utilizes a $RK45$ method). The solutions and their relative errors were then compared. Finally, as the finite difference method proves its utility as a solution to this problem, I compare the computational time versus number of nodes with the accuracy of the interface node versus the number of nodes.

3 Results - Plots

The first plot shown below on the left is the solution obtained using the finite difference method with 25 nodes. Note that the true solution is superimposed on the plot for comparison. The next plot shown is the solution obtained with the first WAG using the shooting method that utilizes $ode45$.

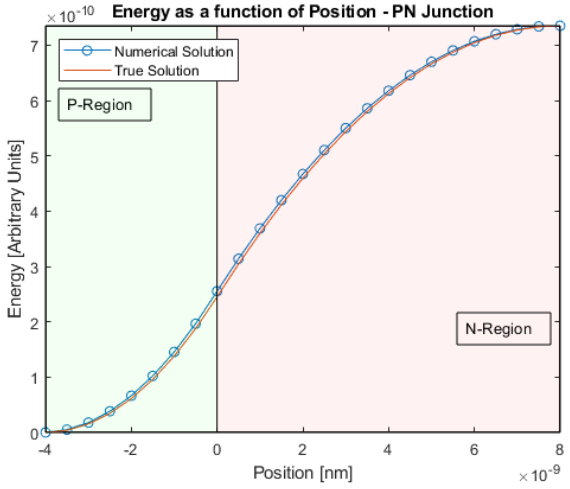

Figure 1: Finite Difference Solution

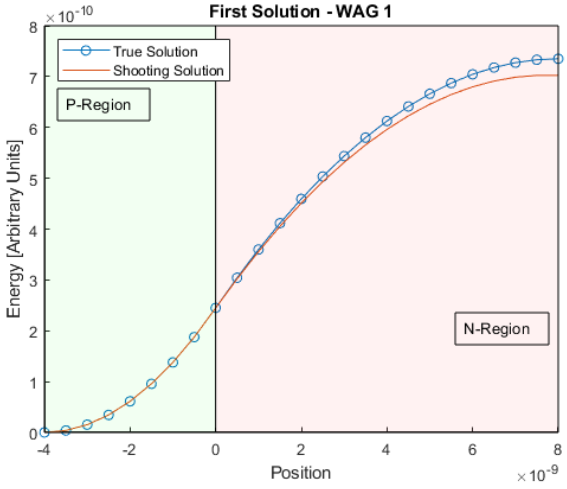

Figure 2: First Shooting Solution

In order to assess the error for each method, the difference between each predicted spatial value and the true value was determined. The absolute error obtained when utilizing the finite difference method is shown below in the figure below on the left. The absolute error obtained after the first shooting iteration is shown below in the figure on the right.

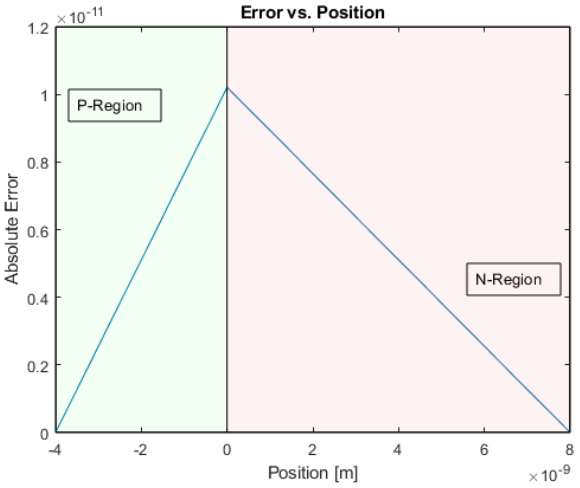

Figure 3: Finite Difference Absolute Error

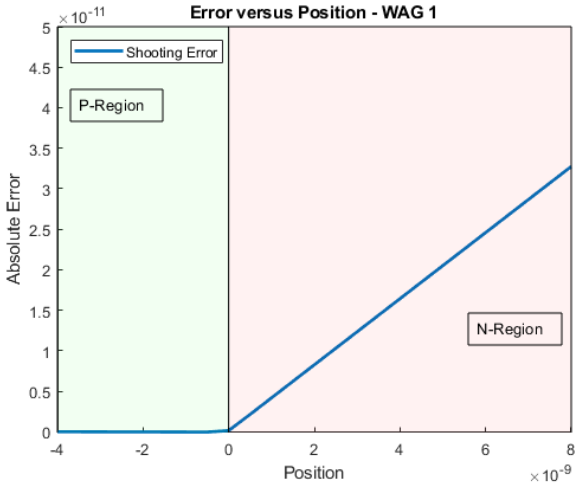

Figure 4: First Shooting Iteration Absolute Error

In order to compare the finite difference method to an alternative numerical method, a shooting solution was implemented. The shooting solution uses *ode*45 to solve the differential equation at each step, and adjusts the boundary condition guess using the secant method; justified by the fact that the ode in question is linear. An animation has been included below to show how the solution changes as each subsequent guess is updated.

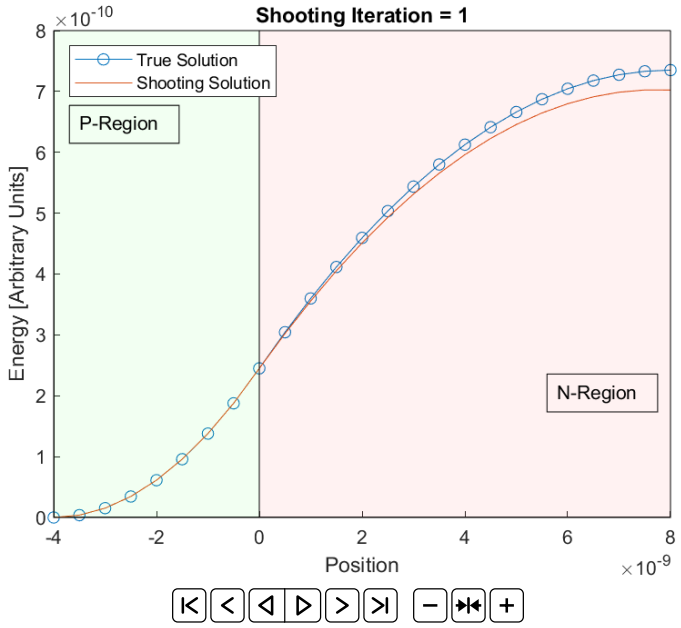

The error of the shooting solution at each step is also shown in an animated plot below.

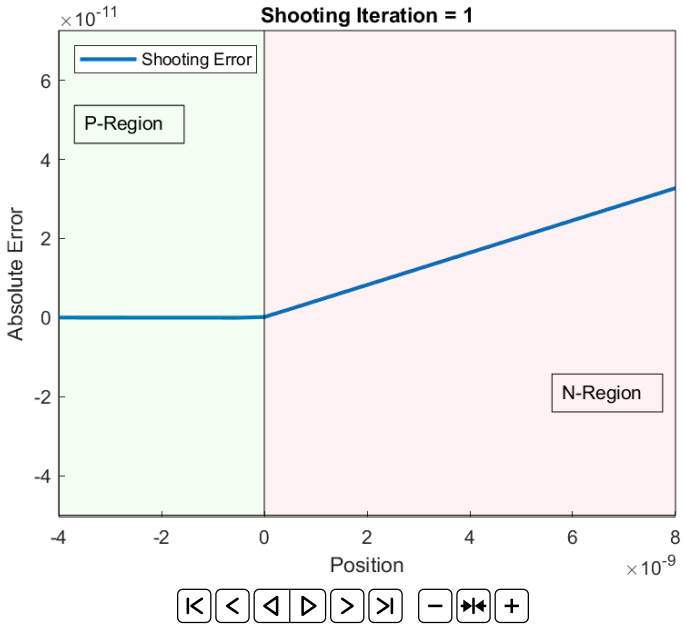

The computational time of each method was examined. Each method was constrained such that there was a maximum error value over the entire spatial region. This choice justifies the comparison of computational time.

```
Elapsed time is 0.001739 seconds.
```

Figure 5: Finite Difference Computational Time

```
Elapsed time is 0.003219 seconds.
```

Figure 6: Shooting Computational Time

Finally, the accuracy of a single node value and the computational time were jointly examined as a function of the number of nodes utilized.

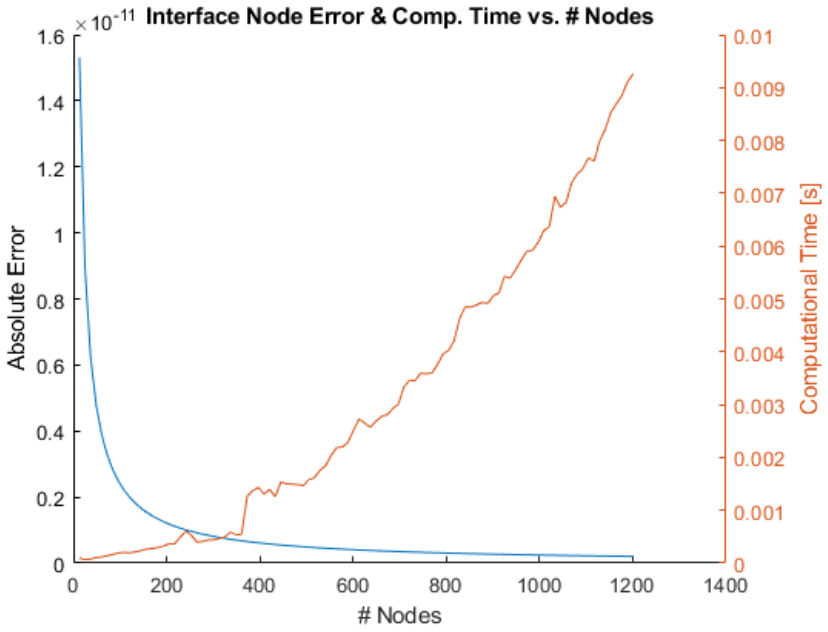

Figure 7: Accuracy & Computational Time vs. # of Nodes

Note that all of the plots shown in this section are discussed in more detail below.

4 Discussion: Numerical vs. Analytical Solution

In order to solve this problem analytically, the solution to Poisson's equation was taken as the appropriately weighted sum of the *Green's Function* solutions. The mathematical details are not very relevant for this report. It should be noted that the solution is not trivial as $\rho(x)$ is a complicated function in reality (not a piece-wise step function as assumed for this problem). However, the assumption that charge carrier density is equal to dopant concentration in each region turns out to be very accurate. Based on the assumptions made in this problem, the second order ODE could be integrated twice with appropriate boundary conditions applied in order to obtain an analytical solution. In order to solve this problem using finite difference approximations, I followed the steps outlined below.

1. Discretized the region of interest
2. Developed nodal equation for a general internal node using finite difference approximations
3. Developed nodal equations for each boundary based on BCs
4. Developed nodal equation for interface node based on continuity condition

In order to solve this problem using the shooting method, I followed the steps outlined below.

1. Reformatted second order ODE as a system of first order ODEs
2. Converted the problem from a BVP to IVP by making a guess for one of the initial BCs (see equation(15))
3. Solved the system of first order ODEs using an RK45 method (*ode*45)
4. Evaluated the error in the predicted boundary node value at the end of the region
5. Repeated steps (3)-(4) with another guess.

6. Utilized a root finding method (the secant method) to drive the error at the last boundary node to zero by intelligently predicting the next guess and repeating steps (3)-(4) until the error was below a predetermined threshold

If one were interested in the variance in the spatial potential in the depletion region as dopant concentrations changed, an appropriate numerical method such as discretization is a much more robust method that could be used to solve this problem for varied depletion region widths and dopant concentrations. Consider the physical relevance of this solution; due to equation (18), the shape of the spatial potential determines how charged particles are effected at a specific position within the depletion region. This information would be useful when determining the movement of generated electron-hole pairs in a photodiode device or photovoltaic device for example, because the movement of charge carriers constitutes a current induced by the incident EM radiation. This is especially important for applications that require very sensitive photo-diodes, such as the Super-Kamioka Neutrino Detection Experiment (see appendix for more information).

5 Discussion: Plots & Error

It is clear from the plots shown above that the finite difference method is a more flexible method for this problem, as the boundary conditions at both ends of the physical medium can properly be accounted for as the carrier concentrations (N_a & N_D) and consequently the depletion widths (d_D & d_A) are varied. When the shooting solution was utilized, the solution obtained at every step using Runge-Kutta methods was very sensitive to the initial guess. Due to the backward-dependent nature of Runge-Kutta methods (RK45 specifically), a poor guess for a boundary condition at the beginning of the region can lead to a large error in the solution value at the other end of the region. As demonstrated, it is possible to use shooting to obtain a solution for this problem, but in general more iterations are required to obtain a reasonable solution. Finite difference methods account for boundary conditions at any point within a discretized region. Therefore, when the problem at hand involves boundary conditions at different locations, finite difference methods are superior when compared to the shooting approach. In addition, shooting methods introduce considerable uncertainty regarding the number of iterations required to obtain an acceptable solution. The number of iterations required can be heavily dependent on the quality of the initial guess, and not every problem is formulated such that it informs the initial guess.

With regard to the error plots, there are several important features to be discussed. It can be seen that the magnitude of the maximum error obtained during the first iteration of the shooting method is $\approx 3\times$ larger than the magnitude of the maximum error obtained using the finite difference method. It should be noted that a stopping criteria for the shooting method was chosen such that the method was halted when the error at the far boundary was less than the maximum spatial error obtained via the finite difference method. In theory, the error of the finite difference method employed to solve this problem is limited to $O(\Delta x)$. Although finite difference equations used for the boundary and general nodal equations were second order accurate ($O(\Delta x^2)$); the interface node required a first-order accurate nodal equation. In order to utilize nodes in the appropriate region for each side of the expression (see equation (13)), the nodal equations required first-order accurate forward & backward difference equations. This step limited the accuracy of the entire finite-difference solution to $O(\Delta x)$. In contrast, the accuracy of the RK45 method utilized by *ode*45 is on the order of $O(\Delta x^4)$. However, due to the failure of *ode*45 to account for boundary conditions properly, the finite difference method is proven superior with regard to this problem. In order to increase the accuracy of the finite-difference solution to $O(\Delta x^2)$, a Crank-Nicholson method could be employed. However, the accuracy was on the order of 10^{-11}, which provides acceptable results for this problem. There is another error artifact worth discussing with regard to the finite difference method; the error is minimized near the boundaries and greatest near the interface node. Due to the spatial inter-dependencies between nodes in the mesh, local errors constituted by truncation error and round-off error have the opportunity to accumulate at nodes farther from the known boundaries. As the error at the interface node between the known boundaries is the maximum error over the entire region; minimizing the error at this node would have the greatest effect on the accuracy of the solution. As discussed earlier, a Crank-Nicholson method could be used to increase the accuracy of the solution at this node to $O(\Delta x^2)$, removing the $O(\Delta x)$ accuracy constraint imposed by first-order accurate finite difference approximations. This accuracy constraint imposed by the boundary node is one of the weaknesses of this particular approach. Note that this constraint was only an issue because there was an interface within the mesh where the differential equation changed. If the behaviour of $U(x)$ spanning the mesh was governed by a single differential equation, the solution could be made second order accurate $O(\Delta x^2)$ without employing the Crank-Nicholson method.

Another important aspect that contributes to the efficacy of each numerical method employed is the computational time. In section (3), it was shown that the computational time required by the shooting solution was $\approx 3\times$ greater than the computational time required by the finite difference method. This is due to the fact that the shooting solution had to solve the same ODE multiple times as the initial boundary condition was updated. In this sense, the shooting method is redundant. As it is clear that the finite difference method is more efficient, it is important to understand the trade-off between accuracy and computational time with regard to the finite difference method. The final plot shown in section (3) shows the accuracy of the interface node as a function of the number of nodes utilized, with the computational time superimposed on the plot. When using the finite difference method, it is clear that there is a point of diminishing returns as the computational time increases linearly but the accuracy approaches a horizontal asymptote. Thus, when using a finite difference method to solve a problem, maximizing the node count is not always ideal. Instead, a decision should be made to limit the number of nodes involved in the simulation such that the desired accuracy is reached without expending unnecessary computational resources.

In conclusion, a finite difference method and a shooting method were both applied to solve the problem outlined in section (1). The finite difference method was shown to be the superior approach in this case, and the efficiency of the finite difference method was examined. In addition, the magnitude of the error of each method was assessed. Finally, the limitations and strengths of the finite difference method were examined in the context of the presented problem.

6 Appendix

If you are having trouble viewing the animations (please use Adobe Acrobat), two .mp4 videos have been uploaded that represent the animations present in this report.

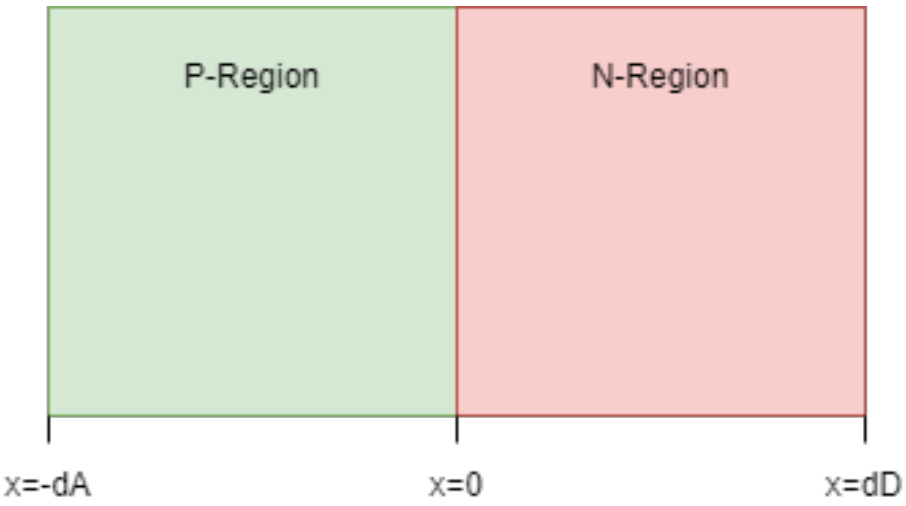

Figure 8: PN Junction Spatial Diagram

Below are the nodal equations obtained by applying finite difference approximations.

General Node (P-Region):

$$\beta U_{i-1} - 2\beta U_i + \beta U_{i+1} = 1 \tag{6}$$

$$\beta = \frac{\epsilon\epsilon_0}{eN_A\Delta x^2} \tag{7}$$

General Node (N-Region):

$$\alpha U_{i-1} - 2\alpha U_i + \alpha U_{i+1} = -1 \tag{8}$$

$$\alpha = \frac{\epsilon\epsilon_0}{eN_D\Delta x^2} \tag{9}$$

First Node Applied Boundary Condition:

$$U_0 = 0 \tag{10}$$

Last Node Applied Boundary Condition:

$$U_n = U(n) \tag{11}$$

Interface Node Applied Boundary Condition:

$$\frac{\partial U_A}{\partial x} = \frac{\partial U_D}{\partial x} \tag{12}$$

$$\frac{U_i - U_{i-1}}{\Delta x} = \frac{U_{i+1} - U_i}{\Delta x} \tag{13}$$

$$-U_{i-1} + 2U_i - U_{i+1} = 0 \tag{14}$$

$$\frac{\partial^2 U}{\partial x^2} = \frac{\rho}{\epsilon\epsilon_0} \text{ becomes } \begin{cases} y_1 = U_x \\ y_2 = y_1' = U_{xx} \end{cases} \tag{15}$$

$$BC_{i+1} = BC_i - \frac{\epsilon_i}{\epsilon_{i-1} - \epsilon_i} \times (BC_{i-1} - BC_i) \tag{16}$$

$$\begin{gathered} N_A = 2 \times 10^{16} \ \frac{holes}{cm^3} \\ N_D = 1 \times 10^{15} \ \frac{e^-}{cm^3} \\ d_A = 4 \times 10^{-9} \ m \\ d_D = 8 \times 10^{-9} \ m \end{gathered} \tag{17}$$

$$F = \frac{-\partial U}{\partial x} \tag{18}$$

More information on the Super-Kamioka Neutrino Experiment can be found here!